Conformational Analysis of a Cyclic RGD Peptide Containing a $\psi[CH_2–NH]$ Bond: A Positional Shift in Backbone Structure Caused by a Single Dipeptide Mimetic

Armin Geyer, Gerhard Müller, and Horst Kessler*

Contribution from the Institut für Organische Chemie und Biochemie, Technische Universität München, Lichtenbergstrasse 4, D-85747 Garching, Germany

Received February 7, 1994®

Abstract: The pseudopentapeptide *cyclo*(-Arg¹-Gly²-Asp³-D-Phe⁴$\psi[CH_2–NH]$Val⁵-) (**1**) was synthesized by a combination of solution and solid-phase methods. The reduced peptide bond was incorporated as a dipeptide building block, a versatile synthetic alternative that avoids the reduction of imine intermediates. NMR spectroscopy was used to investigate the structure of the peptide. Interproton distances from a NOESY spectrum served as restraints in a molecular dynamics simulation. Though the peptide exhibits a typical βII′,γ conformation with the D-Phe in the $i + 1$ position of a γ turn, this solution conformation is different from that of the parent peptide *cyclo*(-Arg¹-Gly²-Asp³-D-Phe⁴-Val⁵-) with the D-Phe in the $i + 1$ position of βII′. The influence of the reduced peptide bond is examined by computational methods. The $\psi[CH_2–NH]$ bond proved to be a strong hydrogen bond donor and thus rigidifies the peptide backbone.

Introduction

The combined approach of design, chemical synthesis, and structural analysis of rigid bioactive peptide analogs allows one to indirectly identify the receptor-bound conformation of functional peptide sequences.[1–4] Incorporation of peptide bond modifications can improve the pharmacokinetics of peptides through increased resistance against proteolytic degradation, even if the modification is located some residues away from a protease-labile bond.[5] The resulting peptide mimetics are intermediates on the path from native peptide sequences to therapeutic agents.[6] Amide bond modifications additionally alter torsional freedom of the backbone and modify hydrogen bond acceptor and donor properties, hydrophobicity, and charge distribution.[7] The comparison of peptide templates with their backbone-modified analogs helps one understand the structural influence of the peptide backbone and its hydrogen bond forming properties.[8] A frequently used nonhydrolyzable isostere for a peptide bond is the so-called *reduced peptide bond* $\psi[CH_2–NH]$. Its chemical realization is feasible even in the course of solid phase peptide synthesis,[9,10] and numerous examples of reduced peptides are being investigated in medical research.[11–14] The incorporation of a reduced amide within a peptide is expected to cause increased backbone flexibility and a loss of hydrogen bond acceptor properties but retains hydrogen bond donating activity and the spatial dimensions of an amide bond.[11,15,16]

In this study we present synthesis and conformational analysis of a reduced amide bond containing cyclic pentapeptide *cyclo*(-Arg¹-Gly²-Asp³-D-Phe⁴$\psi[CH_2–NH]$Val⁵-) (**1**). The dipeptide isostere Boc-D-Phe$\psi[CH_2–NH]$Val-OH served as a building block in solid-phase peptide synthesis. Cyclization was performed by azide activation of the C-terminal carboxylic acid with diphenyl phosphoryl azide in dilute dimethylformamide.[17,18] The trifluoroacetic acid salt of the peptide was studied in the solvent mixture DMSO/water, assuring the protonated state of the reduced peptide bond: $\psi[CH_2–NH_2^+]$. Conformational studies of peptide **1** are based on structurally relevant NMR parameters such as nuclear Overhauser effects (NOEs) extracted from 2D NOESY, vicinal homonuclear coupling constants from E.COSY, and temperature coefficients of main chain NH resonances.[19,20]

Peptide **1** was designed on the basis of the unmodified parent peptide *cyclo*(-Arg¹-Gly²-Asp³-D-Phe⁴-Val⁵-) (**2**), which adopts a βII′,γ conformation according to previously published investigations.[21,22] We will focus on the conformational characteristics of a protonated reduced peptide bond and the predictability of the solution conformation of the modified peptide **1**, which clearly differs from the parent peptide **2**.

We also performed a conformational search with the model compound Ac-D-Ala¹$\psi[CH_2–NH_2^+]$L-Ala²-NHCH₃, which has minimal steric requirements resembling those of the D-Phe⁴ψ-$[CH_2–NH_2^+]$Val⁵ fragment of **1**, to search for energy minima of a $\psi[CH_2–NH_2^+]$ fragment connecting a N-terminal D-residue

* Abstract published in *Advance ACS Abstracts,* July 15, 1994.

(1) Kessler, H. *Angew. Chem., Int. Ed. Engl.* **1982**, *21*, 512–523.
(2) Hruby, V. J. *Life Sci.* **1982**, *31*, 189–199.
(3) Kessler, H. *J. Prakt. Chem.* **1992**, *334*, 549–557.
(4) Hruby, V. J.; Al-Obeidi, F.; Kazmierski, W. *Biochem. J.* **1990**, *268*, 249–262.
(5) (a) Fok, K. F.; Panzer-Knodle, S. G.; Nicholson, N. S.; Tjoeng, F. S.; Feigen, L. P.; Adams, S. P. *Int. J. Peptide Protein Res.* **1991**, *38*, 124–130. (b) Reference 47.
(6) Hirschmann, R. *Angew. Chem., Int. Ed. Engl.* **1991**, *30*, 1278–1303.
(7) Spatola, A. F. In *Chemistry and Biochemistry of Amino Acids, Peptides and Proteins*; Weinstein, B., Ed.; Marcel Dekker: New York, 1983; Vol. 7, pp 267–357.
(8) Kessler, H.; Geyer, A.; Matter, H.; Köck, M. *Int. J. Peptide Protein Res.* **1992**, *40*, 25–40.
(9) Sasaki, Y.; Coy, D. H. *Peptides* **1987**, *8*, 119–121.
(10) Coy, D. H.; Hacart, S. J.; Sasaki, Y. *Tetrahedron* **1988**, *44*, 835–841.
(11) Haffar, B. M.; Hocart, S. J.; Coy, D. H.; Mantey, S.; Chiang, H. V.; Jensen, R. T. *J. Biol. Chem.* **1991**, *266*, 316–322.
(12) Harbeson, S. L.; Shatzer, S. A.; Le, T.; Buck, H. *J. Med. Chem.* **1992**, *35*, 3949–3955.
(13) Kohl, N. E.; Moser, S. D.; deSolms, S. J.; Giuliani, E. A.; Pompliano, D. L.; Graham, S. L.; Smith, R. L.; Scolnick, E. M.; Oliff, A.; Gibbs, J. B. *Science* **1993**, *260*, 1934–1937.
(14) Coy, D. H.; Heinz-Erian, P.; Jiang, N.; Sasaki, Y.; Taylor, J.; Moreau, J.; Wolfrey, W. T.; Gardner, J. D.; Jensen, R. T. *J. Biol. Chem.* **1988**, *263*, 5056–5060.
(15) Marraud, M.; Dupont, V.; Grand, V.; Zerkout, S.; Lecoq, A.; Boussard, G.; Vidal, J.; Collet, A.; Aubry, A. *Biopolymers* **1993**, *33*, 1135–1148.
(16) Dauber-Osguthorpe, P.; Campbell, M. M.; Osguthorpe, D. J. *Int. J. Peptide Protein Res.* **1991**, *38*, 357–377.
(17) Brady, S. F.; Varda, S. L.; Freidinger, R. M.; Schwenk, D. A.; Mendlowski, M.; Holly, F. W.; Veber, D. F. *J. Org. Chem.* **1979**, *44*, 3101–3105.
(18) Brady, S. F.; Paleveda, W. J.; Arison, B. H.; Freidinger, R. M.; Nutt, R. F.; Veber, D. F. *Proceedings of the 8th American Peptide Symposium;* 1983; pp 127–130.
(19) Kessler, H.; Bermel, W.; Müller, A.; Pook, K.-H. In *The Peptides, Analysis, Synthesis, Biology*; Udenfriend, S., Meienhofer, J., Hruby, V., Eds.; Academic Press: New York, 1985; Vol. 7, pp 437–473.
(20) Mierke, D. F.; Kessler, H. *Biopolymers* **1993**, *33*, 1003–1017.
(21) Gurrath, M.; Müller, G.; Kessler, H.; Aumailly, M.; Timpl, R. *Eur. J. Biochem.* **1992**, *210*, 911–921.
(22) Müller, G.; Gurrath, M.; Kessler, H.; Timpl, R. *Angew. Chem., Int. Ed. Engl.* **1992**, *31*, 326–328.

0002-7863/94/1516-7735$04.50/0

Table 1. ^1H and ^{13}C NMR Chemical Shifts (ppm) of Pseudopeptide **1**

	Arg[1]	Gly[2]	Asp[3]	D-Phe[4] [a]	Val[5]
$N^{\alpha}H/N^{\delta}H$	9.77/9.61	8.64	7.40	7.63	
$H^{\alpha}/H^{\alpha'}$	3.72	3.7–3.74	4.65	4.17	3.55
$H^{\beta\ proR}/H^{\beta\ proS}$	1.49/1.85		2.44, 2.77	2.72–2.75	2.07
$H^{\gamma}{}_2/H^{\gamma}{}_3$	1.49[b]				0.9/0.96
$H^{\delta}{}_2$	3.10[b]				
CO	172.45	169.45	171.86	*a*	168.36
C^{α}	55.72	44.81	49.64	48.89	66.89
C^{β}	25.98		36.45	38.18	29.49
$C^{\gamma}/C^{\gamma'}$	26.36				18.4/18.7
C^{δ}	40.74				

[a] Proton chemical shifts for the $C^{red}H_2$ group of the reduced amide bond are 2.73 ppm (*proS*) and 3.40 ppm (*proR*); the ^{13}C chemical shift is 52.88 ppm. [b] Signal overlap.

with a C-terminal L-residue. A conformational shift of the entire backbone structure of **1** in comparison to **2** was not predictable without including the experimental restraints.

Peptides containing the tripeptide sequence Arg-Gly-Asp (RGD) are of current interest in medicinal chemistry. 'RGD-peptides' interfere with a variety of cell–cell and cell–matrix interactions and thus allow a targeted modulation of cellular recognition phenomena such as platelet aggregation or anchorage and migration mechanisms of tumor cells and ostoeclasts (osteoblasts).[23] Positioning and orientation of the ionic side chains of Arg and Asp are essential for selective receptor recognition.[24–27] Thus, the structural investigation of rigid peptide analogs helps one understand the complex biological phenomena mentioned above.

Methods

Synthesis. All solvents were distilled before use, 2-chlorotrityl chloride resin and Fmoc-Asp(O^{t}Bu)-OH were purchased from Novabiochem (Bad Soden), and Lawesson's reagent[28] was purchased from E. Merck (Darmstadt). Analytical and preparative HPLC was performed on NUCLEOSIL 7 C_{18} material (Macherey-Nagel, Düren). The capacity factors k' were determined as described in ref 29. Molecular weight determination was made by fast atom bombardment mass spectroscopy (FAB-MS).

Boc-D-Pheψ[CH$_2$–NH]Val-OH. Boc-D-Phe-Val-OBzl (7.1 g, 15.6 mmol) was reacted for 2 h with 4.5 g (11 mmol, 0.7 equiv) of Lawesson's reagent in 50 mL of refluxing tetrahydrofurane. The reaction mixture was dissolved in ethyl acetate and extracted against saturated $NaHCO_3$. Crude Boc-D-Pheψ[CS–NH]Val-OBzl was obtained in nearly quantitative yield. The reaction was monitored by ^1H NMR (δ, DMSO-d_6, CSN*H* = 10.1 ppm).

Boc-D-Pheψ[CS–NH]Val-OBzl (7 g, 15 mmol) and 29.7 g (125 mmol) of $NiCl_2 \cdot 6H_2O$ were dissolved in 100 mL of tetrahydrofuran/MeOH (1/1 v/v), the mixture was cooled to 0 °C, and 14.5 g (374 mmol) of $NaBH_4$ was added in small portions. After 30 min, the reaction mixture was separated from undissolved reaction products by suction over Celite, and the solvent was evaporated on a rotary evaporator. The dry gray mass was resuspended in ethyl acetate and the peptidic fraction extracted from the solid. After flash chromatography (ethyl acetate/hexane on silica gel 60, E. Merck), the Boc-D-Pheψ[CH$_2$–NH]Val-OBzl crystallized. Yield: 3.5 g (8 mmol = 53%). ^1H NMR (δ, DMSO-d_6) 0.85 (t, 6H, Val H^{γ}), 1.3 (s, 9H, Boc), 1.8 (m, 1H, Val H^{β}), 2.3, 2.6, 2.8 (dd, m, dd, J = 5.3 and 13.2 Hz, 4H, D-Phe H^{β}, D-Phe $C^{red}H_2$), 2.95 (d, J = 6.1 Hz, 1H, Val H^{α}), 3.55–3.75 (m, 1H, D-Phe H^{α}), 5.1 (s, 2H, benzyl-CH_2), 6.55 (d, J = 9 Hz, 1H, D-Phe NH), 7.1–7.4 (m, 10H, arom); mp = 57 °C; $[\alpha]^{20}_D$ = –7.4 (c 0.5, MeOH).

The C-terminus was deprotected by catalytic hydrogenation in MeOH with 10% Pd/C catalyst over 30 min (TLC control). The peptide was used in solid-phase peptide synthesis without further purification. FAB-MS 373 (M + Na^+).

H-D-Pheψ[CH$_2$–NH]Val-Arg(NO$_2$)-Gly-Asp(OBzl)-OH·2TFA. Fmoc-Asp(OBzl)-OH (1 g, 2.1 mmol) was coupled to 0.7 g of 2-chlorotrityl chloride resin (1.4–1.6 mmol/g) by standard methods described in the literature.[30] H-Arg(NO_2)-Gly-Asp(OBzl)-2-chlorotrityl resin was synthesized in two deprotection (20% piperidine in CH_2Cl_2) and coupling cycles (3 equiv of *O*-(1*H*-benzotriazol-1-yl)-*N*,*N*,*N*′,*N*′-tetramethyluronium tetrafluoroborate (TBTU) and 3 equiv of Fmoc-protected amino acid in 30mL of 1-methyl-2-pyrrolidone) on a semiautomatic peptide synthesizer (SP 650 Labortec).

Boc-D-Pheψ[CH$_2$–NH]Val-OH (0.2 g, 0.6 mmol) was coupled with 0.5 g (1.5 mmol) of TBTU in 30 mL of 1-methyl-2-pyrrolidone for 1 h. The linear pseudopentapeptide was cleaved from the resin and simultaneously deprotected at its N-terminus with 30 mL of TFA/H_2O/thioanisol (27.5/1.5/1 v/v/v). Yield = 0.47 g (0.5 mmol), k' = 4.33, gradient of H_2O/MeCN (80:20 to 40:60) over 20 min. Cyclization of the linear peptide was performed without further purification.

***cyclo*(-D-Pheψ[CH$_2$–NH]Val-Arg(NO$_2$)-Gly-Asp(OBzl)-)·TFA.** Cyclization of 250 mg (0.27 mmol) of linear pseudopeptide was performed in 150 mL of dimethylformamide with 0.16 mL (0.7 mmol) of diphenyl phosphoryl azide and 100 mg (1.2 mmol) of $NaHCO_3$ as a solid base over 24 h. The solvent was evaporated and the oil solidified upon suspension in water. The crude product was separated and rinsed with ether.

FAB-MS 696 (M + H^+). Yield = 170 mg (0.21 mmol = 80%), k' = 5.2, gradient of H_2O/MeCN (80:20 to 40:60) over 20 min. ^1H NMR (δ, DMSO-d_6) 0.82 (m, 6H, Val H^{γ}), 1.5, 1.7–1.85 (m, 4H, Arg H^{β}, Arg H^{γ}), 1.75 (m, 1H, Val H^{β}), 2.4, 2.6–2.7 (m, 5H, D-Phe H^{β}, D-Phe CH_2, Val H^{α}), 2.5, 2.9 (m, 2H, Asp H^{β}), 3.15 (m, 1H, Arg H^{δ}), 3.5, 3.9 (m, 2H, Gly H^{α}), 3.95 (m, 1H, D-Phe H^{α}), 4.1 (m, 1H, Arg H^{α}), 4.8 (m, 2H, Asp H^{α}), 5.0 (s, 2H, benzyl-CH_2), 7.02 (d, J = 8.2 Hz, 1H, D-Phe NH), 7.1–7.3 (m, 10 H, arom), 7.95 (d, J = 10 Hz, 1H, Asp NH), 8.35 (dd, J = ca. 5 Hz, 1H, Gly NH), 8.45 (d, J = 8.6 Hz, 1H, Arg NH).

***cyclo*(-D-Pheψ[CH$_2$–NH]Val-Arg-Gly-Asp-) (1).** Final deprotection was performed by catalytic hydration of 170 mg (0.2 mmol) of cyclic pseudopeptide with 350 mg of dry 10%Pd/C catalyst in 15 mL of dry MeOH.

FAB-MS 561 (M + H^+), yield = 100 mg (0.18 mmol = 80%), k' = 0.15, gradient of H_2O/MeCN (80:20 to 40:60) over 40 min.

Final purification was performed by preparative HPLC. Further data for **1** are given in Tables 1and 2.

NMR. Spectra were recorded on Bruker AC 250 and AMX 500 spectrometers and processed on Bruker X32 computers with UXNMR software. The sample contained 10 mg (13 μmol) of *cyclo*(-Arg-Gly-

Table 2. Temperature Dependence of Amide Protons between 300 and 340 K (–ppb/K) and Proton Vicinal Coupling Constants (Hz) of Pseudopeptide **1**

	Arg[1]	Gly[2]	Asp[3]	D-Phe[4] [a]	Val[5]
$\Delta\delta/\Delta T$	7.5	5	<1	3.5	
$^3J(NH,H^{\alpha})$	7.2	Σ = 12.1	9.2	8.9	
$^3J(H^{\alpha},H^{\beta})$		*b*	7.1, 7.3	*b*	6.5

[a] $^3J(H^{\alpha},C^{red}H^{proR}) < 1$ Hz; $^3J(H^{\alpha},C^{red}H^{proS}) = 9$ Hz. [b] Signal overlap.

(23) (a) Rouslahti, E.; Pierschbacher, M. D. *Science* **1987**, *238*, 491–497. (b) Hynes, R. O. *Cell* **1992**, *69*, 11–25.
(24) Dennis, M. S.; Carter, P.; Lazarus, R. A. *Proteins: Struct., Funct., Genet.* **1993**, *15*, 312–321.
(25) O'Neil, K. T.; Hoess, R. H.; Jackson, S. A.; Ramachandran, N. S.; Mousa, S. A.; DeGrado, W. F. *Proteins: Struct., Funct., Genet.* **1992**, *14*, 509–515.
(26) Rao, S. N. *Peptide Res.* **1992**, *5*, 148–155.
(27) Cotrait, M.; Kreissler, M.; Hoflack, J.; Lehn, J.-M.; Maigret, B. *J. Comput.-Aided Drug Des.* **1992**, *6*, 13–130.
(28) Clausen, K.; Thorsen, M.; Lawesson, S.-O. *Bull. Soc. Chim. Belg.* **1981**, *37*, 3635–3639.
(29) Hearn, M. T. W., Ed.; *HPLC of Peptides, Proteins and Polynucleotides*; VCH Publishers, Inc.: New York, 1991.
(30) Barlos, K.; Gatos, D.; Kallistis, J.; Papahotiu, G.; Soririu, P.; Wenqing, Y.; Schäfer, W. *Tetrahedron Lett.* **1989**, *30*, 3943–3946.

Asp-D-Pheψ[CH_2–NH]Val-) (**1**) as a trifluoroacetic acid salt dissolved in 0.5 mL of DMSO-d_6/water (80/20 v/v), degassed in several pump and freeze cycles. Chemical shifts are calibrated to the DMSO-d_6 solvent signal at 2.5 ppm for ^{1}H and 39.5 ppm for ^{13}C. All spectra were recorded at 300 K except for the spectra for temperature coefficient measurement, which were measured in 10 K steps from 300 to 340 K. All spectra except the HMQC-TOCSY were recorded with 4K data points in f_2 and 512 t_1 experiments.

The TOCSY spectrum[31,32] was recorded with 40 scans per t_1 increment at a proton frequency of 250 MHz. Presaturation of the solvent signal was performed during the relaxation delay of 1 s. The spectral width was 3697 Hz and the mixing time was 44 ms, flanked by two 2.5-ms trim pulses.

Two NOESY spectra[33] were recorded with 40 scans per t_1 increment at 500.14 MHz and different mixing times of 100 and 175 ms. The spectral width was 6329 Hz, and the relaxation delay was 1.5 s. Solvent suppression was achieved by the 1–1 jump return method.[34] After zero filling, the size of the matrix was 4096 × 2048 data points. Apodization with a squared cosine bell function was used in both dimensions, and the baseline was corrected after Fourier transformation. The intensities of cross peaks were measured by the integration routine within the UXNMR program.

The E. COSY spectrum was recorded on the AC 250 as described in refs 35 and 36 with 512 t_1 increments, 4K data points, and a spectral width of 2000 Hz; using presaturation of the solvent signal.

The HMQC with TOCSY transfer[37,38] was recorded with 24 scans per t_1 increment at 500.14 MHz (125.76 MHz for ^{13}C) with a spectral width of 7042 Hz in f_2 (^{1}H) and 6322 Hz in f_1 (^{13}C). 256 experiments were recorded with a mixing time of 40 ms, and the solvent was presaturated during the relaxation delay of 1.2 s. GARP decoupling was performed during acquisition.

Computational Procedure. All modeling studies and molecular mechanics simulations were carried out on Silicon Graphics 4D/25TG, 4D/70GTB, 4D/240SX, and 4D/Crimson computers. For all interactive modeling and graphical display, the program INSIGHT-II (Biosym Technologies Inc., San Diego, CA) was used. In MD simulations utilizing the programs of the Groningen Molecular Simulation Software Package (GROMOS[39]), the constrained Verlet method (SHAKE[40]) was applied with a relative tolerance of 10^{-4}, which allowed an integration time step of 2 fs. Since SHAKE is not implemented in the DISCOVER program package, the integration time step was set to 1 fs for all molecular dynamics calculations utilizing the consistent valence force field.[41] The initial velocity vectors assigned to all atoms of the system in MD simulations were taken from a Maxwellian distribution resembling the desired temperature.

The D-Phe^4–Val^5 peptide bond of the refined structure of **2** was manually converted to the ψ[CH_2–NH_2^+] reduced amide isostere within INSIGHT-II, without remarkably altering the peptide backbone conformation. This interactively generated structure served as starting conformation for three molecular dynamics simulations performed at temperatures of 300, 600, and 1200 K, respectively, without inclusion of experimentally derived restraints. The calculations were carried out using the consistent valence force field implemented in DISCOVER without any cross terms. A dielectric constant of 78 was used in order to minimize long-range Coulomb interactions that are overemphasized in vacuum simulations. All three MD simulations covered 500 ps, and the trajectories were updated every 500 steps, yielding ensembles of 1000 structures for each temperature.

The dipeptide model Ac-D-Ala^1ψ[CH_2–NH_2^+]L-Ala^2-$NHCH_3$ was constructed with INSIGHT-II. The two sp^3-centers of the reduced peptide bond allowed three staggered low-energy conformations for the pseudo-ω dihedral angle: +60°, –60°, and 180°. The conformational characteristics of the model peptide were studied for the rotamers in three independent simulations by systematically incrementing the ψ dihedral angle of D-Ala^1 and the ϕ dihedral angle of L-Ala^2 in 10° steps. The low-energy conformations were identified by variation of the torsions that flank the reduced amide bond. All other main-chain torsion angles of the model peptide adopted a fully extended conformation. The simulations for each reduced amide conformer included 1296 different conformations.

The NMR-based final structure refinement for **1** was performed with GROMOS. Two different starting structures were generated interactively. Both starting structures were minimized by 500 steps of steepest descent in order to remove strain caused by the model-building procedure. After energy minimization a high-energy molecular dynamics simulation was performed covering 5 ps at a system temperature of 1000 K, followed by 10 ps at 500 K and 20 ps at 300 K with a strong coupling to an external heat bath (τ_T = 0.01 ps). During this vacuum simulation all charges of the side-chain functionalities of Arg^1 and Asp^3 were scaled down to zero to avoid artificial back-folding tendencies of these side chains due to overemphasized electrostatic forces.[42] The charges of the backbone NH groups were scaled down according to the measured temperature coefficients of the NH resonances.[43] For this initial phase of the refinement procedure only distance restraints between backbone protons were included in the potential energy function with a harmonic term scaled by a force constant k_{dr}, which was set to 4000 kJ·mol^{-1}·nm^{-2}.[44,45] The conformers obtained after this high-temperature simulation were minimized using the conjugate gradients method and served as starting structures for subsequent solvent simulations applying periodic boundary conditions. As the NMR investigations were carried out in a DMSO/water solvent *mixture*, which is not parametrized within GROMOS, we studied the dynamics of both starting conformations in two different solvent environments, namely pure water[46] and pure DMSO.[47] Both starting structures were soaked in a water box of about 3.8 Å box-length, containing approximately 860 solvent molecules, and in a DMSO box of 4.0 Å box-length, consisting of about 260 solvent molecules, respectively. In both simulations, the solvent shell was allowed to relax over 1000 steps of energy minimization while the peptide was tethered. Over an additional 1000 steps, the complete system was energy minimized to derive starting conditions for the subsequent MD simulations. All MD calculations in the solvent boxes were performed at 300 K over a period of 150 ps. During the first 50 ps all NMR-derived distance restraints were included with a force constant to k_{dr} = 1000 kJ·mol^{-1}·nm^{-2}. From 50 to 100 ps the restraining potential was decreased with k_{dr} = 500 kJ·mol^{-1}·nm^{-2} while the last 50 ps were simulated without any restraining potential. This free dynamics simulation was carried out to make sure that the NMR-derived conformation obtained after 100 ps of restrained MD remains stable and therefore represents a low-energy conformation in the physical force field.[48]

Results

Synthesis. Pseudopeptide **1** was synthesized according to the reaction scheme shown in Figure 1.

Biological Activity. The two peptides **1** and **2** inhibit the binding of fibrinogen and of the extracellular matrix protein vitronectin to the isolated integrin $\alpha_v\beta_3$. Linear H-Gly-Arg-Gly-Asp-Ser-OH inhibits the binding of vitronectin to the isolated integrin $\alpha_v\beta_3$ with an IC_{50} of 750 nM. The cyclic parent peptide **2** shows strongly increased activity (50 nM) and selectivity.[49] The activity of **1** lies between both peptides (E. Merck, unpublished results).

(31) Braunschweiler, L.; Ernst, R. R. *J. Magn. Reson.* **1983**, *53*, 521–528.
(32) Bax, A.; Davies, D. G. *J. Magn. Reson.* **1985**, *65*, 355–360.
(33) Jeener, J.; Meier, B. H.; Bachman, P.; Ernst, R. R. *J. Chem. Phys.* **1979**, *71*, 4546–4553.
(34) Gueron, M.; Plateau, P.; Decorps, M. *Prog. NMR Spectrosc.* **1991**, *23*, 135–210.
(35) Griesinger, C.; Sørensen, O. W.; Ernst, R. R. *J. Am. Chem. Soc.* **1985**, *107*, 607–609.
(36) Griesinger, C., Sørensen, O. W.; Ernst, R. R. *J. Chem. Phys.* **1986**, *85*, 6837–6852.
(37) Lerner, L.; Bax, A. *J. Magn. Reson.* **1986**, *69*, 375–380.
(38) Byung-Ha, O.; Westler, W. M.; Markley, J. L. *J. Am. Chem. Soc.* **1989**, *111*, 3083–3085.
(39) van Gunsteren, W. F.; Berendsen, H. J. C. *GROMOS, Groningen Molecular Simulation (GROMOS) Library Manual*; Nijenborgh: Groningen, Germany, 1987; pp 1–227.
(40) van Gunsteren, W. F.; Berendsen, H. J. C. *Mol. Phys.* **1977**, *34*, 1311–1327.
(41) Dauber-Osgythorpe, P.; Roberts, V. A.; Osgythorpe, D. J.; Wolff, J.; Genest, M.; Hagler, A. T. *Proteins: Struct., Funct., Genet.* **1988**, *4*, 31–47.
(42) Kurz, M.; Mierke, D. F.; Kessler, H. *Angew. Chem., Int. Ed. Engl.* **1992**, *31*, 210–212.
(43) Kessler, H.; Bats, J. W.; Griesinger, C.; Koll, S.; Will, M.; Wagner, K. *J. Am. Chem. Soc.* **1988**, *110*, 1033–1049.
(44) van Gunsteren, W. F.; Berendsen, H. J. C. *Angew. Chem., Int. Ed. Engl.* **1990**, *29*, 992–1023.
(45) Brünger, A. T.; Karplus, M. *Acc. Chem. Res.* **1991**, *24*, 54–61.
(46) Berendsen, H. J. C.; Postma, J. P. M.; van Gunsteren, W. F.; Hermans, J. In *Intermolecular Forces*; Pullman, B., Ed.; Reidel: Dordrecht, The Netherlands, 1981; pp 331–342.
(47) Mierke, D. F.; Kessler, H. *J. Am. Chem. Soc.* **1991**, *113*, 9466–9470.
(48) Saulitis, J.; Mierke, D. F.; Byk, G.; Gilon, C.; Kessler, H. *J. Am. Chem. Soc.* **1992**, *114*, 4818–4827.
(49) Pfaff, M.; Tangemann, K.; Müller, B.; Gurrath, M.; Müller, G.; Kessler, H.; Timpl, R.; Engel, J. *J. Biol. Chem.*, submitted.

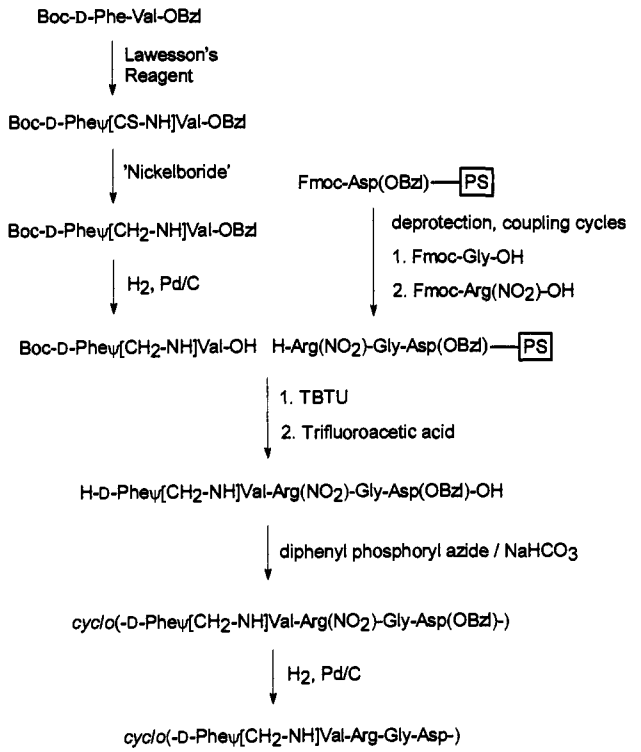

Figure 1. Synthesis of peptide **1**. Further details are given in the experimental part.

NMR. All studies were performed in a DMSO-d_6/water mixture.[50] We observed no significant changes in chemical shifts compared to those of a solution of **1** in pure DMSO-d_6 and exclude a solvent-dependent conformational rearrangement. The wide dispersion of chemical shifts, the significant difference in temperature gradients, and the separation of diastereotopic geminal protons of up to 1 ppm (CH_2 of the reduced peptide bond) indicate low probability for conformational averaging on the ^{1}H NMR time scale. This 'cryoprotective mixture'[51,52] of DMSO/water is suitable for low-temperature measurements. We did not observe significant line broadening even at temperatures as low as 270 K.

Exchangable protons like the NH_2^+ group of the reduced peptide bond and the guanidinium group could not be assigned due to the broad signals caused by fast chemical exchange.

The ^{1}H NMR signals were assigned with a TOCSY spectrum and a HMQC-TOCSY spectrum. The geminal protons of D-Phe $C^\beta H_2$ and the CH_2 protons of the reduced peptide bond could be distinguished by the ^{13}C NMR shift of 38.2 ppm for the side-chain CH_2 and 53.0 ppm for the main-chain CH_2 group (Table 1).

The low-field shift values (9.87 ppm) and the temperature coefficient of –7.5 ppb/K for the Arg NH are typical for solvent exposed amide protons. In contrast, the Asp NH resonates at the highest field of all amide protons (7.40 ppm) with the smallest temperature coefficient of <–1 ppb/K, indicating a solvent-shielded NH, typical for amide protons involved in intramolecular hydrogen bonds (Table 2).

Interproton distances were obtained by integration of cross peaks from the NOESY spectrum with 175-ms mixing time. Distances used as restraints for the computer simulations are listed in Table 3.

$^3J(NH,H^\alpha)$ coupling constants were derived from a 1D-spectrum. $^3J(H^\alpha,H^\beta)$ and $^3J(H^\alpha,H^{red})$ coupling constants were extracted from an E. COSY spectrum and are listed in Table 2. Side-chain coupling constants were only determined for Asp and Val.

Conformational Search. In order to study the conformational consequences of the CONH to CH_2–NH_2^+ modification between the two amino acids D-Phe^4 and Val^5, we altered the affected peptide bond within the previously analyzed MD structure of **2**.[21] The backbone conformation of **2** is characterized by a βII′,γ turn arrangement (Figure 2), stabilized by a pair of hydrogen bonds between the main-chain functionalities of Arg^1 and Asp^3. D-Phe^4 is found in the $i+1$ position of the βII′ turn, while the $i+1$ position of the γ turn is occupied by Gly^2 (Figure 2). In this structure, the central peptide bond of the βII′ turn was replaced, resulting in the starting structure for the MD simulations (Figure 3). The CO and NH functionalities of that particular amide bond are not involved in any turn-stabilizing intramolecular hydrogen bonds in the refined conformation of *cyclo*(-Arg^1-Gly^2-Asp^3-D-Phe^4-Val^5-) (**2**).[21]

With this artificially generated structure, we carried out three molecular dynamics simulations at 300, 600, and 1200 K to investigate the conformational influence of a reduced peptide bond. A long simulation period of 500 ps was chosen to ensure that the interactively manipulated structure was not trapped in a local energy minimum on the hypersurface of conformational energy. We discuss in detail the results of the MD run at 600 K, representative for all three MD simulations. The dihedral angle of the pseudopeptide bond is exclusively found in the 180° conformation with an *antiperiplanar* relation of the D-Phe^{4}C$^\alpha$ and Val^{5}C$^\alpha$, although the two *gauche* conformers represent low-energy states, too. A similar restriction is observed for the two flanking torsions, the pseudo-ψ dihedral of D-Phe^4, defined by N–C$^\alpha$–CH_2–NH_2^+ (denoted as ψ(D-Phe) in the following), and the pseudo-ϕ dihedral of Val^5, defined by CH_2–NH_2^+–C$^\alpha$–C (denoted as ϕ(Val)), of the dipeptide isostere backbone. Both torsions fluctuate moderately around an equilibrium value. The pseudopeptide bond prefers a 180° torsion, comparable to a native peptide bond in *trans* configuration. This locally conserved feature cannot be observed for the main-chain structure of the entire peptide. The experimentally derived conformation for the parent peptide **2** is not stable during the dynamics simulation. The β turn-stabilizing hydrogen bond oscillates between 2.5 and 7.4 Å, and the γ turn-stabilizing hydrogen bond fluctuates between 1.8 and 5.1 Å, respectively. This indicates the exploration of a wide conformational space in the free dynamics simulations of the modified peptide **1**, modeled on the experimentally refined structure of **2**.

Thus, this theoretical study suggests a preferred local conformation within the dipeptide isostere D-Phe$^4\psi$[CH_2–NH_2^+]Val^5, namely a *transoid* conformation for the pseudo-ω dihedral. Furthermore, it was not possible to define a preferred global backbone structure, as no major populated conformational family could be analyzed throughout the course of all three dynamics simulations.

Ac-D-Ala$^1\psi$[CH_2–NH_2^+]L-Ala^2-NHCH$_3$ mimics on a minimal structural level the dipeptide isostere of **1**. The N- and C-terminal capping groups avoid terminal charge effects and mimic the preceeding and succeeding peptide chain. Alanine was used for both amino acid positions as a simple side-chain-bearing residue. Systematical variation of the ψ(D-Ala) and ϕ(Ala) torsions by 10° increments demonstrated a highly restricted conformational space for the +60° and –60° staggered rotamers of pseudo-ω with respect to the flanking dihedral angles. Wide areas of the ψ/ϕ map are excluded due to atom overlap. The antiperiplanar orientation (pseudo-ω = 180°) of the dipeptide isostere D-Ala$^1\psi$-[CH_2-NH_2^+]L-Ala^2 restricts only the ϕ dihedral angle of L-Ala^2 (Figure 4). ϕ values between –60° and +60° give rise to high-energy conformations caused by repulsive interactions between the L-Ala^2 carbonyl group and the methylene group of the

(50) Motta, A.; Picone, D.; Tancredi, T.; Temussi, P. A. *Tetrahedron* **1988**, *44*, 975–990.
(51) Fesik, S. W.; Olejniczak, E. T. *Magn. Reson. Chem.* **1987**, *25*, 1046–1048.
(52) Motta, A.; Picone, D.; Tancredi, T.; Temussi, P. A. *J. Magn. Reson.* **1987**, *75*, 364–370.

Table 3. Experimentally Derived Distance Restraints That Were Used as Upper and Lower Bounds for Structure Refinement in Restrained Molecular Mechanics Simulations of **1**[a]

proton A	proton B	r^{upper}	r^{lower}	I	II	III	IV	V	VI
Arg^1NH	Arg^1H^{α}	237	215	218	226	223	227	223	220
Arg^1NH	$Arg^1H^{\beta}_2$	411	299	364	318	331	364	361	367
Arg^1NH	Val^5H^{α}	237	213	214	208	206	211	212	211
Arg^1NH	Val^5H^{β}	384	348	403	417	407	412	423	419
Arg^1NH	D-$Phe^4C^1H_2$	405	300	376	331	362	347	321	328
Arg^1H^{α}	$Arg^1H^{\beta\ proS}$	252	228	255	300	295	246	254	249
Arg^1H^{α}	$Arg^1H^{\beta\ proR}$	252	228	300	252	262	298	298	301
Gly^2NH	Asp^3NH	273	247	249	252	242	279	275	256
Gly^2NH	$Gly^2H^{\alpha}_2$	315	225	245	242	247	238	238	243
Gly^2NH	$Arg^1H^{\beta}_2$	295	205	211	260	248	199	203	207
Asp^3NH	D-Phe^4NH	242	200	276	266	279	261	259	287
Asp^3NH	Asp^3H^{α}	289	263	288	292	292	292	292	292
Asp^3NH	$Asp^3H^{\beta\ proR}$	326	294	309	290	287	373	364	371
Asp^3NH	$Asp^3H^{\beta\ proS}$	326	294	326	310	319	259	246	258
Asp^3NH	$Arg^1H^{\beta}_2$	415	283	421	421	420	392	413	421
Asp^3H^{α}	$Asp^3H^{\beta proR}$	284	257	301	302	301	256	265	258
Asp^3H^{α}	$Asp^3H^{\beta\ proS}$	284	257	255	254	249	301	302	299
D-Phe^4NH	Asp^3H^{α}	281	255	251	263	252	278	287	255
D-Phe^4NH	D-Phe^4H^{α}	309	279	292	294	293	293	293	290
D-Phe^4NH	D-$Phe^4C^1H_2$	329	220	301	318	309	319	321	324
Val^5H^{α}	D-$Phe^4C^1H_2$	324	234	241	248	241	254	255	253
Val^5H^{α}	Val^5H^{β}	264	238	310	309	298	308	309	310
average restraint violation				8	8	10	12	12	12

[a] The corresponding distances out of different conformations are given to prove the quality of the refined structures. Columns I–III contain distances from three representatives of the simulations in DMSO and columns IV–VI in water. All distances in ppm.

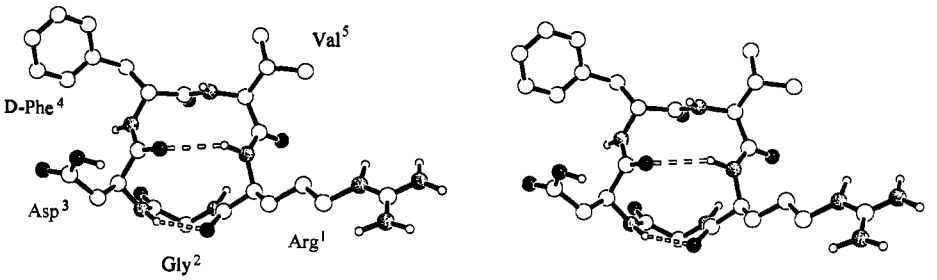

Figure 2. Stereoview of *cyclo*(-Arg^1-Gly^2-Asp^3-D-Phe^4-Val^5-) (**2**) from refs 21 and 22. Hydrogen bonds are indicated by dotted lines.

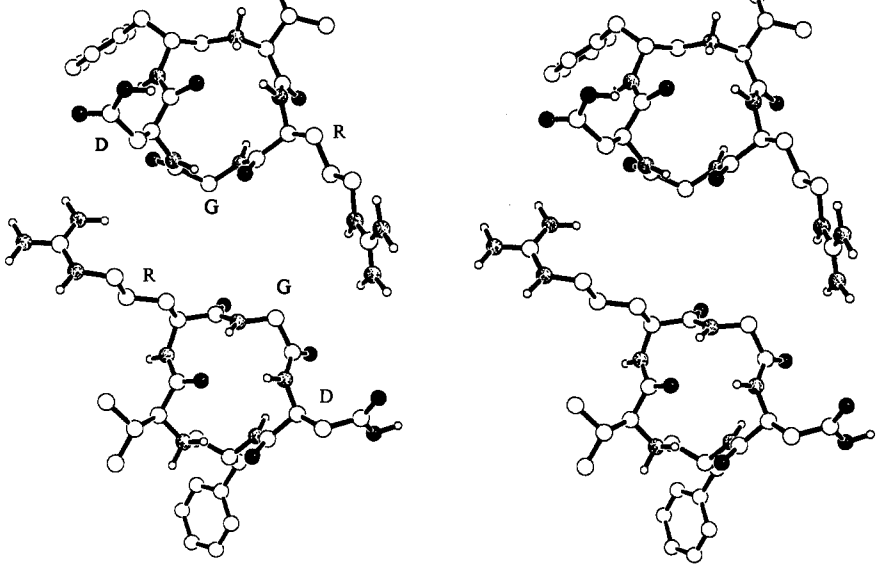

Figure 3. Stereoviews of the two starting structures for the MD simulation of *cyclo*(-Arg^1-Gly^2-Asp^3-D-$Phe^4\psi[CH_2–NH_2^+]Val^5$-) (**1**). The structure shown above is derived from the solution structure of **2**, with the amide bond between D-Phe^4 and Val^5 exchanged by a protonated reduced peptide bond. Below, a second starting structure with D-Phe^4 positioned in the $i + 1$ position of the γ turn is shown.

pseudopeptide bond. The minimum-energy conformational areas for pseudo-$\omega = 180°$ are analyzed for ψ(D-Ala) around −70° and −170° and for ϕ(L-Ala) around −160° and −90° in the lower left part of the ψ/ϕ map.

Thus, a conformational search with an unconstrained linear model peptide supports the free dynamics simulations of the cyclic pentapeptide discussed above. Local conformational preference of the dipeptide isostere can be observed, but no structure for the entire backbone of **1** could be derived from these modeling studies.

The *experimentally* based structure elucidation of **1** was carried out utilizing restrained molecular mechanics simulations starting with two different initial structures. The starting structure in

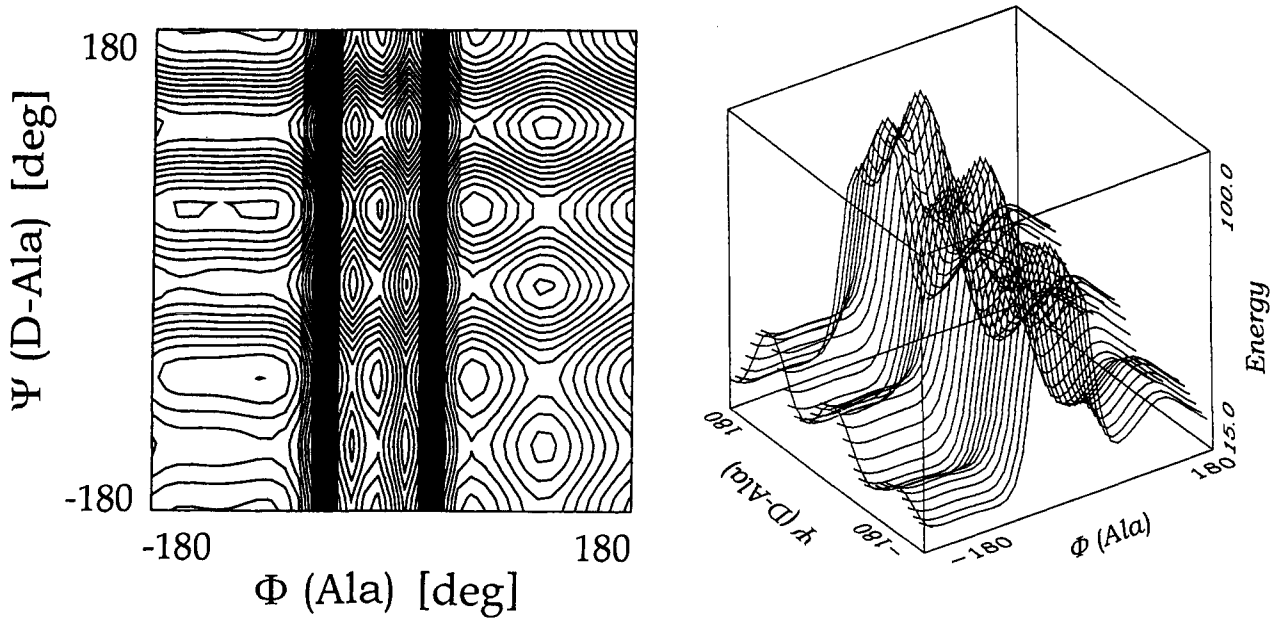

Figure 4. Ramachandran-like plot and corresponding energy profile of the protonated reduced dipeptide model Ac-D-Ala$^1\psi$[CH_2-NH_2^+]Ala^2-$NHCH_3$.

Table 4. Dihedral Angles (deg) of the Snapshots of **1** during the MD Simulations in DMSO and in Water

residue	torsion	80DMSO	120DMSO	150DMSO	75water	125water	150water	**2**[a]
	ϕ	58	57	62	53	51	57	−128
Arg^1	ψ	−96	−100	−90	−120	−109	−98	73
	ω	180	179	175	178	178	175	−179
	ϕ	−86	−81	−94	−63	−65	−78	88
Gly^2	ψ	−24	−26	−35	−32	−35	−46	−66
	ω	−174	−176	−172	−174	−175	−173	169
	ϕ	−149	−130	−123	−114	−110	−108	−85
Asp^3	ψ	69	50	59	40	28	52	81
	ω	174	175	178	175	−179	178	−172
	ϕ	109	101	103	103	108	95	85
D-Phe^4	ψ	−73	−65	−71	−64	−60	−64	−111
	ω	148	143	148	141	141	146	178
	ϕ	−82	−70	−75	−70	−68	−69	−58
Val^5	ψ	134	120	129	121	111	116	−46
	ω	175	176	176	−176	−175	−179	−178

the upper part of Figure 3 resembles the refined solution conformation of the parent peptide **2**, and the second starting structure (lower part of Figure 3) was modeled in accordance with the low-temperature coefficient of Asp^{3}NH (Table 2), an obvious sign of internal orientation and formation of a hydrogen bond. Furthermore, this structure takes into account the positional preferences for characteristic turn positions of glycine and amino acids in the D-configuration. Glycine adopts the $i + 2$ position of a β turn,[21,53,54] whereas D-Phe is the central residue of a γ turn. Positional preferences of residues in the D-configuration within cyclic oligopeptides are well documented in the literature,[21,53-55] and both starting structures meet these preferences completely.

The backbone conformations for both structures showed an identical turn arrangement after minimization. This vacuum-derived structure served as starting system for two independent restrained MD simulations in DMSO and in water. Backbone dihedral angles of three snapshots from the trajectories in the two different solvents are given in Table 4. Comparing the different sets of dihedral angles, all three structures fluctuate around common equilibrium conformations. This equilibrium conformation is substantially different from the formerly NMR-refined structure of the parent peptide **2**. This is most obvious

Table 5. Hydrogen Bond Analysis over Fractions of Trajectories of the MD Simulations of **1** in DMSO and Water[a]

donor	acceptor	r_{D-A} (pm)	r_{H-A} (pm)	θ_{D-H-A} (pm)	population (%)	turn type
		DMSO (40–80 ps)				
Asp^{3}NH	Val^{5}CO	308	214	159	99	βII′
Val^5NH_2^+	Asp^{3}CO	334	243	151	83	γ
		Water (25–75 ps)				
Asp^{3}NH	Val^{5}CO	321	242	138	62	βII′
Val^5NH_2^+	Asp^{3}CO	337	250	148	82	γ

[a] Further details are given in the text.

for the tripeptide fragment Val^5-Arg^1-Gly^2. The solvent simulations were carried out with all distance restraints included during the first 100 ps of the 150-ps simulation period. Distances for three conformations out of each simulation are given in Table 3. These conformations were obtained by averaging over certain time intervals and minimization. The DMSO-derived structures meet the distance restraints slightly better than the water-derived structures. The average restraint violations for I and II are 4 pm smaller than the corresponding values for IV and V. Again, the backbone structures are nearly identical. Nevertheless, the slightly better reproduction of the experimental data by simulation of **1** in a DMSO environment is supported by the hydrogen bond analysis over the two trajectories (Table 5). While the γ turn around D-Phe^4 is stabilized by a hydrogen bond between the protonated secondary amine of the dipeptide mimetic and Asp^3-CO in both simulations, the β turn formed by Val^5-Arg^1-Gly^2-

(53) Sherman, D. B.; Spatola, A. F. *J. Am. Chem. Soc.* **1990**, *112*, 433–441.
(54) Bean, J. W.; Kopple, K. D.; Peishoff, C. E. *J. Am. Chem. Soc.* **1992**, *114*, 5328–5334.
(55) Kostansek, E. C.; Thiessen, W. E.; Schomburg, D.; Lipscomb, W. N. *J. Am. Chem. Soc.* **1979**, *101*, 5811–5815.

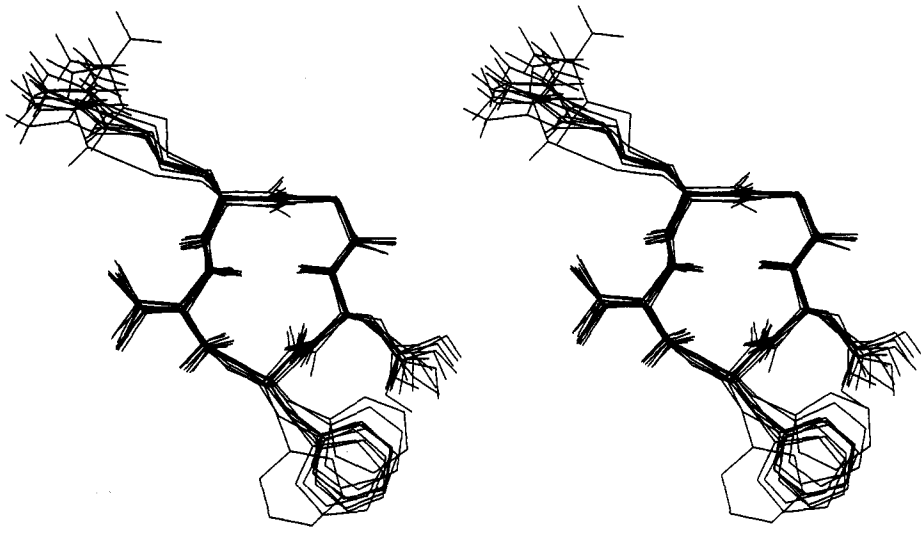

Figure 5. Ten representative conformations of the restrained MD simulation of **1** in DMSO.

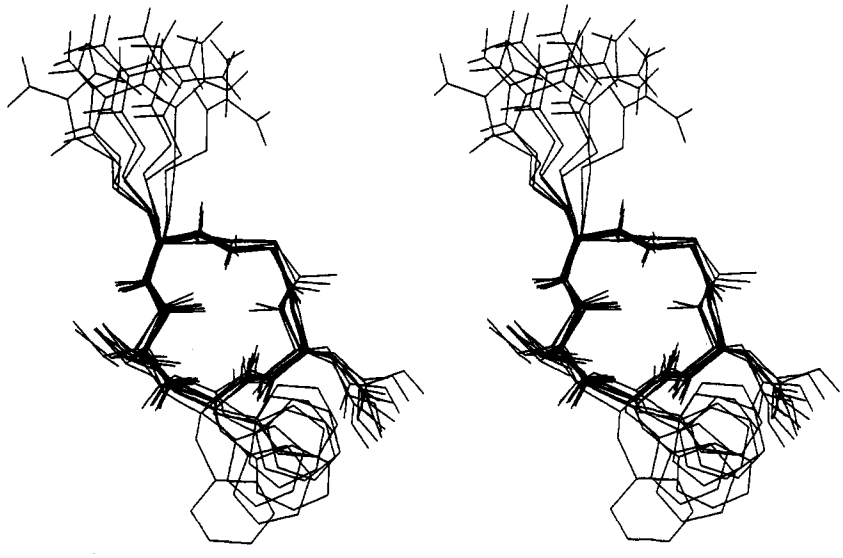

Figure 6. Ten representative conformations of the MD simulation of **1** in DMSO without experimental restraints. The principal backbone structure is conserved, but the increased flexibility in comparison to Figure 5 is obvious.

Asp^3 is described by a far higher populated transannular hydrogen bond between Asp^3NH and Val^5CO over the DMSO trajectory. The less populated hydrogen bond during the water simulation can be rationalized in terms of peptide–water interactions. Water molecules interact as donors with main-chain carbonyl groups and are acceptors for hydrogen bonds with main-chain amide protons. This competing effect of formation of intermolecular hydrogen bonds over intramolecular interactions explains the lower population of the $Asp^3NH \rightarrow Val^5CO$ hydrogen bond as compared to the case of the monofunctional DMSO environment and may furthermore account for the moderately enhanced agreement of the DMSO-derived conformations with the experimentally obtained distances. Therefore in the following sections we focus on a detailed conformational analysis of structures derived from the DMSO trajectory.

A superposition of 10 snapshots taken from the DMSO simulation every 5 ps between 50 and 100 ps clearly supports a conserved backbone conformation throughout the restrained MD run (Figure 5) and is in agreement with the experimental results. The structure is characterized by a βII′ turn with Arg^1 and Gly^2 in the central positions and an intramolecular hydrogen bond between Asp^3NH and Val^5CO. D-Phe^4 is found in the $i + 1$ position of a γ turn stabilized by the second observed hydrogen bond between $Val^5NH_2^+$ and Asp^3CO. The βII′ turn is well defined by interproton distances derived from 2D NOESY cross-peak intensities (Table 3). The Asp^3NH is found in close proximity to Gly^2NH, which accounts for an exposure of both amide protons to the same direction relative to the peptide backbone. The correlation of the Asp^3NH to the Arg^1H^β protons and the lack of correlation between Gly^2NH and Arg^1H^α indicate opposite orientation of Gly^2NH and Arg^1H^α with respect to the peptide ring plane. The modified pseudopeptide bond is now included as a donor in the γ turn-defining hydrogen bond and links the $i + 1$ with the $i + 2$ residue of the regular γ turn. This is additionally supported by the vicinal coupling constants of D-Phe H^α to the two geminal protons of the reduced peptide bond $^3J(H^\alpha, H^{red\ proR})$ and $^3J(H^\alpha, H^{red\ proS})$ of <1 and 9 Hz (Table 2). The corresponding dihedral angles from the simulation in DMSO are −77.1° for $H^{red\ proR}$ and 162.9° for $H^{red\ proS}$. In order to ensure that the NMR-derived peptide conformation of **1** is a meaningful low-energy conformation in the unbiased physical force field, we followed the dynamics over a further 50 ps in the solvent environment. Figure 6 shows a structural superposition of 10 snapshots, taken in 5-ps intervals from the unrestrained fraction of the MD simulation in DMSO. It is not surprising that the dynamical fluctuations are increased, since the artificially included interproton distances restrict the motional and dynamical freedom in a restrained MD run. Nevertheless, the refined backbone conformation remains stable over the monitored simulation period. Figure 7 shows the conformation of **1** after the DMSO simulation

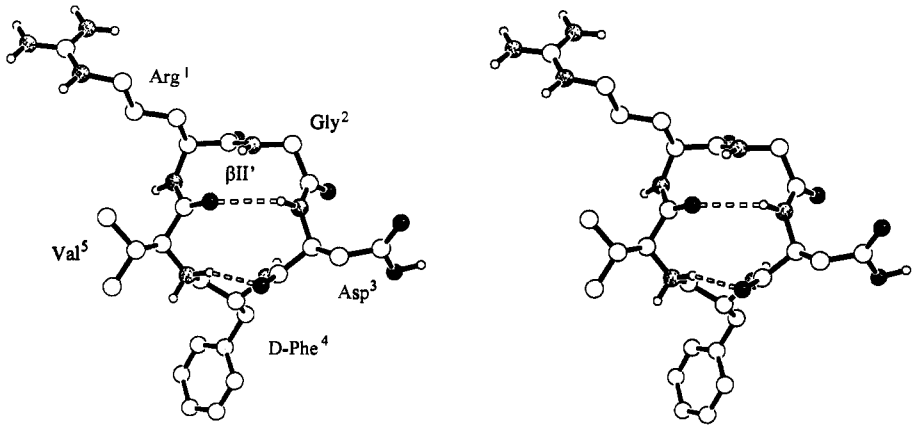

Figure 7. Stereoview of the averaged conformation of *cyclo*(-Arg¹-Gly²-Asp³-D-Phe⁴ψ[CH_2–NH_2^+]Val⁵-).

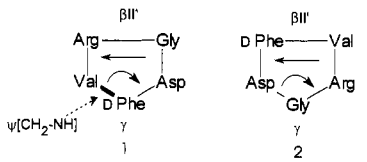

Figure 8. Schematic representation of the two different backbone strucures of *cyclo*(-Arg¹-Gly²-Asp³-D-Phe⁴ψ[CH_2-NH_2^+]Val⁵-) and the parent peptide *cyclo*(-Arg¹-Gly²-Asp³-D-Phe⁴-Val⁵-).

with the hydrogen bonds indicated, and backbone structures of **1** and **2** are schematically shown in Figure 8.

Discussion

Chemical access to reduced peptides is feasible in two different ways. Reductive alkylation of resin-bound peptide amines with Boc-protected amino (acid) aldehydes in the presence of $NaBH_3CN$ allows relatively easy access to incorporation of a reduced amide bond into a peptide backbone.[10] Still, the formation of diastereomeric peptides due to apparent racemization of the C^α atom of the Boc-amino aldehyde component was observed in several cases.[56-59] This epimerization depends not only on the optical purity of the Boc-amino aldehyde but also on the reaction conditions, the excess of $LiAlH_4$, and the flanking amino acids. After cleavage from the resin, epimerization of a C^α atom in a longer peptide is difficult to detect and to separate. A second access to reduced amide bonds is provided by the reduction of thiopeptides.[60] Bock et al.[61] demonstrated the potential of this method by incorporating a reduced peptide bond into a natural cyclic hexapeptide. Regioselective thionation offered the possibility of investigating the peptide with a ψ[CO–NH], with a ψ[CS–NH], and with a ψ[CH_2–NH] bond. The regioselectivity of O/S exchange in a peptide larger than a dipeptide is not predictable, and the selective synthesis of thiopeptides is not yet a standard method.[62,63]

Alternatively a reduced dipeptide building block can be incorporated within a peptide via solid-phase peptide synthesis as described in this article. Though the synthesis of protected reduced dipeptide isosters yields typically only about 50% of the desired product,[64] these pseudopeptides are free of racemization and can be crystallized. Their use in solid-phase peptide synthesis is straightforward due to their lack to racemization. The nitrogen of the secondary amine functionality of reduced peptide bonds needs no protection during coupling; exceptions are described in the literature for Gly.[64]

In a solvent mixture of DMSO-d_6/water (8/2 v/v) for NMR studies, the nitrogen atom of the ψ[CH_2–NH] bond exists as a quaternary ammonium ion. A rigidification of the peptide backbone was described in several cases,[64] even in the comparison to the unmodified parent peptide.[65] The ability of protonated reduced peptide bonds to stabilize turns was recently described by Marraud et al.[15] In the case of peptide **1**, the restriction of conformational freedom becomes obvious in Figure 4.

Comprehensive conformational search studies on reduced amide links in model peptides were published by P. Dauber-Osguthorpe et al.[16] A general result is that the C-terminal amino acid of a reduced amide containing dipeptide isostere can adopt nearly any conformation. Thus, a peptide bond reduction should be compatible with common types of β turns and more stable conformations are obtained when the central amide bond or the one between the $i + 2$ and $i + 3$ positions is substituted.

Simulating the reduced peptide bond under physiological conditions, i.e. in the protonated state, the ψ[CH_2–NH_2^+] moiety in **1** proved to be unexpectedly restricted in terms of torsional freedom, even at high simulation temperatures. The rest of the peptide explores a wide range of conformational space; thus, the restricted values of ψ(D-Phe) and pseudo-ω(D-Phe) not only are caused by the overall restraint of backbone cyclization but also are mostly inherent in the dipeptide mimetic.

Superpositions of snapshots taken from the restrained and free dynamics trajectories confirm the highly restricted dynamical behavior of the peptide backbone which is in contrast to the general effect expected for a CO–NH → CH_2–NH_2^+ substitution (Figure 5). A remarkable result of the conformational study of **1** based on NMR-derived parameters is the positional shift of the primary sequence by two positions in a counterclockwise direction when compared to the parent peptide structure (Figure 8). The L-Xaa-Gly sequence is in the central part of a βII' turn, whereas a βII turn would be expected for this array of amino acids. This positional shift is unexpected, because the structural requirements of the two central amino acids in a βII' turn, i.e. $\phi_{i+1} \approx 60°$, $\psi_{i+1} \approx -120°$, $\omega_{i+1} \approx 180°$, $\phi_{i+2} \approx -80°$, $\psi_{i+2} \approx 0°$, could easily be fulfilled by the investigated dipeptide mimic, especially when taking into account the tolerance of ±30° commonly analyzed for the φ and ψ dihedrals. Such a shift of the reduced amide bond

(56) Ho, P. T.; Chang, D.; Zhong, J.; Musso, G. F. *Peptide Res.* **1993**, *6*, 10–12.
(57) Cushman, M.; Oh, Y. *J. Org. Chem.* **1991**, *56*, 4161–4167.
(58) Harbeson, S. L.; Shatzer, S. A.; Le, T.; Buck, H. *J. Med. Chem.* **1992**, *35*, 3949–3955.
(59) Sasaki, Y.; Murphy, W. A.; Heiman, M. L.; Lance, V. A.; Coy, D. H. *J. Med. Chem.* **1987**, *30*, 1162–1166.
(60) Guziec, F. S.; Wasmund, L. M. *Tetrahedron Lett.* **1990**, *31*, 23–26.
(61) Bock, M. G.; DiPrado, R. M.; Williams, P. D.; Pettibone, D. J.; Clineschmidt, B. V.; Ball, R. G.; Veber, D. F.; Freidinger, R. M. *J. Med. Chem.* **1990**, *33*, 2323–2326.
(62) Unverzagt, C.; Geyer, A.; Kessler, H. *Angew. Chem., Int. Ed. Engl.* **1992**, *31*, 1229–1230.
(63) Hoeg-Jensen, T.; Jakobsen, M. H.; Olsen, C. E.; Holm, A. *Tetrahedron Lett.* **1992**, *32*, 7617–7620.
(64) Elst, P. V.; Elseviers, M.; de Cock, E.; Marsenille, M.; Tourwe, D.; van Binst, G. *Int. J. Peptide Protein Res.* **1986**, *27*, 633–642.
(65) Delaet, N. G. J.; Verheyden, P. M. F.; Tourwe, D.; van Binst, G.; Davis, P.; Burks, T. F. *Biopolymers* **1992**, *32*, 957–969.

from the $(i + 1)$–$(i + 2)$ position into the $(i - 1)$–i position of the βII′ turn is found in a further cyclic pentapeptide investigated in 1993 by S. Ma and A. F. Spatola.[66] They analyzed the cyclic pseudopentapeptide *cyclo*(-Gly¹-Pro²ψ[CH₂–NH]Gly³-D-Phe⁴-Pro⁵-) in different solvent environments and in different protonation states of the secondary amine by means of NMR spectroscopy. The main conformation of the pseudopentapeptide in DMSO forms a βII′ turn involving Gly³-D-Phe⁴-Pro⁵-Gly¹ and contains a *cis* Gly¹–Pro² peptide bond. Apart from the *cis* peptide bond, this backbone conformation matches fairly well our structural result for **1**. The reduced amide bond is found in the same position relative to the common βII′ turn within a cyclic pentapeptide.

The local conformation of the reduced amide bond in the refined structure of peptide **1** turns out to be identical to the predictions derived by the theoretical modeling studies based either on the free dynamics simulations of the modified structure of **2** or on the systematic search studies of the model peptide Ac-D-Ala¹ψ-[CH₂–NH₂⁺]L-Ala²-NHCH₃. The pseudo-ω flanking dihedral angles are found in exactly that part of the calculated Ramachandran-like map in Figure 4, where the absolute minimum area of the conformational energy is found. A slight deviation is analyzed for the pseudo-ω dihedral, which adopts values around 150°, instead of the idealized *transoid* rotamer. This deviation from planarity can be assigned to the electrostatic attraction between one of the positively polarized hydrogen atoms attached to the pseudopeptide nitrogen atom and the carbonyl oxygen atom of Asp³. This interaction induces a moderate deviation of the pseudo-ω dihedral from the 180° conformer in favor of an optimized Θ_{N-H-O} hydrogen bond angle.

Pseudo-ω dihedrals of reduced peptide bonds are well determined in X-ray structures of protein–inhibitor complexes. The X-ray structure of the HIV-1 protease complexed with the reduced amide bond containing inhibitor MVT-101, Ac-Thr¹-Ile²-Nle³ψ-[CH₂–NH]Nle⁴-Gln⁵-Arg⁶-NH₂, refined at 2.3-Å resolution shows the P_1 residue Nle³ in a γ_l conformation with $\phi = -92°$ and $\psi = 72°$.[67] The conformation of the P_1 residue of H-D-His¹-Pro²-Phe³-His⁴-Phe⁵ψ[CH₂–NH]Phe⁶-Val⁷-Tyr⁸-OH complexed in the active site of rhizopuspepsin, refined at 1.8-Å resolution, adopts a comparable inverse γ conformation (ϕ(Phe⁵) = –99°, ψ(Phe⁵) = 59°).[68] In this investigation the authors analyze an intrainhibitor hydrogen bond which is in absolute agreement with the γ turn-stabilizing hydrogen bond in **1**. The secondary amine of the inhibitor is identified in a protonated cationic state and acts as a bifunctional hydrogen bond donor to one of the catalytically active Asp side chains of the enzyme (Asp²¹⁸O^δ2) and intramolecularly to the main-chain carbonyl group of His⁴ in the P_2 position. The rhizopuspepsin inhibitor contains a L-Phe as the $i + 1$ residue, which is found in an inversed γ conformation. The cyclic pentapeptide **1** contains a D-Phe in the same position, which is found in a regular γ conformation, which is a locally restricted mirror image of the corresponding fragment of the inhibitor conformation. This difference of γ turn type can easily be rationalized by inversion of the chirality of residue $i + 1$. Furthermore, the pseudo-ω dihedral angle is found at 129° for the rhizopuspepsin inhibitor, which agrees with the deviation from planarity as discussed for the same dihedral in the discussed conformation of **1**, too. Multiple intermolecular interactions between the subsites of the protease S_i and the inhibitor residues P_i bias the conformational preferences of the inhibitor structure. Nevertheless, we estimate these structural analogies as indirect support of the γ turn conformation found for the tripeptide fragment Asp³-D-Phe⁴ψ[CH₂–NH₂⁺]Val⁵ in the pseudopeptide structure presented in this investigation.

Conclusion

The incorporation of a reduced dipeptide as a building block in solid-phase peptide synthesis offers an alternative to the widely used Boc-amino aldehyde method and is a useful synthetic approach in more cases than just those where epimerization of the Boc-amino aldehyde component is observed.

Though the incorporation of a reduced peptide bond into the backbone of a peptide is only a minor and locally restricted modification, the altered hydrogen bond forming properties can be of major influence on the entire peptide backbone conformation. Under physiological conditions, a reduced peptide bond can rigidify the peptide backbone. The protonated state ψ[CH₂NH₂⁺] acts as a donor for hydrogen bonds and demonstrates turn-stabilizing properties.

This study demonstrates the importance of using experimental results as restraints for computer simulations, even for small and conformationally restricted peptides containing structure-inducing elements such as glycine and residues in the D-configuration.

Acknowledgment. The Deutsche Forschungsgemeinschaft and the Fonds der Chemischen Industrie are gratefully acknowledged for financial support. The RGD project is supported by E. Merck, Darmstadt.

(66) Ma, S.; Spatola, A. F. *Int. J. Peptide Protein Res.* **1993**, *41*, 204–206.
(67) Miller, M.; Schneider, J.; Sathyanarayana, B. K.; Toth, M. V.; Marshall, G. R.; Clawson, L.; Selk, L.; Kent, S. B. H.; Wlodawer, A. *Science* **1989**, *246*, 1149–1152.
(68) Suguna, K.; Padlan, E. A.; Smith, C. W.; Carlson, W. D.; Davies, D. R. *Proc. Natl. Acad. Sci. U.S.A.* **1987**, *84*, 7009–7013.